

Diagnostic Evaluation of Carbon Tetrachloride-induced Rat Hepatic Cirrhosis Model

GI-PPEUM LEE, WON-IL JEONG, DA-HEE JEONG,
SUN-HEE DO, TAE-HWAN KIM and KYU-SHIK JEONG

*Department of Veterinary Pathology, College of Veterinary Medicine,
Kyungpook National University, Daegu 702-701, Korea*

Abstract. *Background:* To find a non-invasive method of diagnosing hepatic fibrosis and cirrhosis, we evaluated the relationship of the hepatic cirrhosis grade between histopathology and mean grey level (MGL) in B-mode ultrasonography in CCl₄-induced liver cirrhosis. *Materials and Methods:* Three groups of rats were treated with olive oil, CCl₄, and CCl₄ + silymarin. Rats were sacrificed at weeks 4, 8 and 12, after B-mode ultrasonography examination, and then analyzed histopathologically for fatty change and fibrosis. *Results:* On the grade of fibrosis, the CCl₄ group showed higher value at 8 and 12 weeks than the silymarin group. However, the fatty change was enhanced in the silymarin group, compared with the CCl₄ group. The B-mode histogram values were the highest in the silymarin group, but the collagen rate was highest in the CCl₄-treated group, at week 12. These results suggest that the B-mode histogram can be more affected by infiltration of lipid than by intact accumulation of collagen fibers. *Conclusion:* In the histogram of 8 and 12 weeks, there were significant differences between the CCl₄-treated group and silymarin group in mean grey levels of B-mode ultrasonography. The histogram of B-mode mean grey level has a close correlation with fatty change and is useful for the diagnosis of liver fibrosis by histopathological analysis.

The liver, which is the major organ responsible for the metabolism of drugs, toxic chemicals and byproducts endogenous to the body, is also the primary target organ for detoxication of many endogenous and exogenous toxic chemicals (1, 2). Therefore, the prevalence of major liver diseases, such as non-alcoholic and alcoholic fatty liver,

chronic hepatitis, fibrosis, cirrhosis or hepatic carcinoma, has been noted and leads to fatal diseases in both human beings and animals (3). Hepatic fibrosis has been noted as a response to necrosis and inflammations caused by various factors such as infection, intoxication, endogenous and exogenous detrimental factors, and leads to the activation of Kupffer cells, mononuclear cells and hepatic stellate cells resulting in the degeneration of hepatic cords. Ongoing necrosis of hepatocytes that overwhelm the hepatic regeneration capacity can be followed by replacement with fibrotic connective tissue (4). Diffuse hepatic fibrosis is known to result in the altered reconstruction of the lobular parenchyma with widespread connective tissue septa, which are circumscribed as a regenerative nodule of hepatocytes and anastomoses between vascular channels linking portal and central vessels (5). Cirrhosis represents the end stage of various infectious, toxic and other forms of hepatic injury (6).

To date, as an accurate diagnostic evaluation, histopathological examination by liver biopsy is the key diagnostic examination for liver cirrhosis (5) but, in clinical practice, the use of liver biopsy has several limitations, such as sample errors, with an estimate mean of 24% of false-negative in series of blind liver biopsy, and complications (7, 8).

Recently, several indirect diagnostic tests for cirrhosis have been evaluated. Diverse markers included either clinical signs (9, 10), ultrasonographic signs (11), and endoscopic and blood biochemical parameters (10). In human medicine, Lun-Genlu *et al.* (12) reported a relationship between grading and staging of hepatic fibrosis and non-invasive diagnostic parameters, including the B-mode ultrasound examination. They reported that there is a very close correlation between liver fibrosis and inflammatory activity. The grading and staging of liver fibrosis are closely related to serum markers, ultrasonography, computed tomography (CT), and/or magnetic resonance imaging (MRI) (12). Particularly imaging technologies such as ultrasonography, CT and MRI could provide useful information (13-15). Among them,

Correspondence to: Kyu-Shik Jeong, Department of Veterinary Pathology, College of Veterinary Medicine, Kyungpook National University, Daegu, 702-701, Korea. Tel: +81-053-950-5975, Fax: +81-053-950-5955, e-mail: jeongks@mail.knu.ac.kr

Key Words: Hepatic cirrhosis, diagnosis of cirrhosis, CCl₄.

ultrasonography has become the most common and valuable method because of its low cost, easy performance and high acceptability by the patient (16, 17).

Chronic liver damage induced by carbon tetrachloride (CCl₄) in rats produces liver fibrosis and biochemical and histological patterns that resemble human liver cirrhosis (18). Thus, the rat model of liver cirrhosis has been useful in studying the effects of hepatoprotective drugs with therapeutic potential for use in humans (19). CCl₄ is one of the most widely used hepatic toxins for experimental induction of liver fibrosis and cirrhosis following hepatocellular necrosis in laboratory animals. Besides hepatocellular regeneration and inflammatory infiltration, hepatocellular regeneration, proliferation of hepatic stellate cells and deposition of connective tissue are major features of liver histopathology after 6 ~ 9 weeks of intoxication by CCl₄ (20).

The flavonoid silymarin [Legalon R], which occurs in the thistle *Silybum marianum* (L), was introduced as a "hepatoprotective" agent a few years ago (21, 22). In experimental animals, this flavonoid exerts a protective action on the liver, which is particularly effective in poisoning by several hepatotoxic substances, for example CCl₄, thioacetamide and D-galactosamine (23). Silymarin is a potent anti-oxidant that inhibits lipid peroxide formation in liver cells (24, 25), and which has anti-inflammatory activities mediated by the alteration of hepatic Kupffer cell function (26).

Thus, the primary objective of the current study was to evaluate the correlation between the B-mode histogram of liver parenchyma and histopathological fibrotic change in CCl₄-induced cirrhosis and pathological grading of fibrosis and cirrhosis with silymarin by histopathological examination, and to optimize the value of liver ultrasonography examination as a diagnostic method for the prognosis of cirrhosis treatments.

Materials and Methods

Animals and treatments. Studies were performed on forty-five male Wistar rats, weighing 130 ~ 150 g. They were housed in a room at 22±2°C and 12 hours light dark cycle and were given food and water *ad libitum*. Fibrosis/cirrhosis was induced by intraperitoneal injection of 1.0 ml/kg body weight of 10% CCl₄ in olive oil as a vehicle, three times a week for 12 weeks. Three groups of 15 animals each were used. These groups are schematically shown in Table I. The first group received olive oil 1.0 ml/kg intraperitoneal injection (*i.p.*) three times a week and 0.25% CMC (carboxymethylcellulose) 1.0 ml/kg per oral 5 days a week for 12 weeks. The second group received CCl₄ 1.0 mg/kg, *i.p.* and 0.25% CMC per oral administration (*p.o.*). In addition to CCl₄, the third group received a daily oral dose of 50 mg/kg silymarin 5 times a week. Silymarin was given as a suspension in 0.25% CMC. Five rats of each group were sacrificed at weeks 4, 8 and 12, respectively.

Ultrasonographic examination. On the day of ultrasonograms and sacrifice in every 4 weeks, all rats were transported to the

Table I. *Animals and experimental designs.*

Group	Numbers	Treatments
Control	15	Olive oil (<i>i.p.</i>) + 0.25% CMC* (<i>p.o.</i>)
CCl ₄ **	15	CCl ₄ ^{a)} (<i>i.p.</i>) + 0.25% CMC (<i>p.o.</i>)
Silymarin + CCl ₄	15	CCl ₄ (<i>i.p.</i>) + Silymarin ^{b)} (<i>p.o.</i>)

CMC*: Carboxymethylcellulose

CCl₄** : Carbon tetrachloride

a): 10% CCl₄ in olive oil 1 ml/kg, intraperitoneal injection (*i.p.*)

b): 50 mg/kg silymarin in 0.25% CMC 1 ml/kg, per oral administration (*p.o.*)

Table II. *Comparison of histopathological results and fibrosis grades.*

Weeks	Groups	Hepatic lobular lesion (H&E)	Grade of fibrosis* (Azan)
4 weeks	Control	Normal	0
	CCl ₄	Fibrosis (mild)	5
	Silymarin + CCl ₄	Fatty change (mild)	0-1
8 weeks	Control	Normal	0
	CCl ₄	Fibrosis (severe)	3
	Silymarin + CCl ₄	Fatty change & Fibrosis (mild)	1-2
12 weeks	Control	Normal	0
	CCl ₄	Cirrhosis	4
	Silymarin + CCl ₄	Fatty change & Fibrosis (severe)	2-3

*Fujiwara *et al.*, 1988.

Grade 0: none

Grade 1: short collagenous septa extend from central veins

Grade 2: slender septa link the central veins but lobular architecture is preserved

Grade 3: pseudolobuli form thin septa

Grade 4: parenchyma is subdivided into pseudolobuli by thin septa

laboratory and, using Medison SONOACE9900 Prime with 11MHz (L5-12IM) linear probe, ultrasonographic examination was performed on all experimental groups and on weeks 4, 8 and 12, before each animal sacrifice, respectively. Following anesthesia with xylazine (Rompun®, Bayer Corp., Shawnee Mission, KS, USA) and ketamin (Ketara®, Yu-han Pharm Co. Kyounggido, Korea), the hair on the cranial abdomen was shaved for liver scanning. B-mode ultrasonographic scanning was performed on the median and left lateral lobes. From the abdominal skin to the liver parenchyma, 1cm depth was fixed and then the occurrence frequency of grey levels was described as a number for the 1cm, three limited square for liver parenchymal histogram on weeks 4, 8 and 12, before animals were sacrificed, respectively.

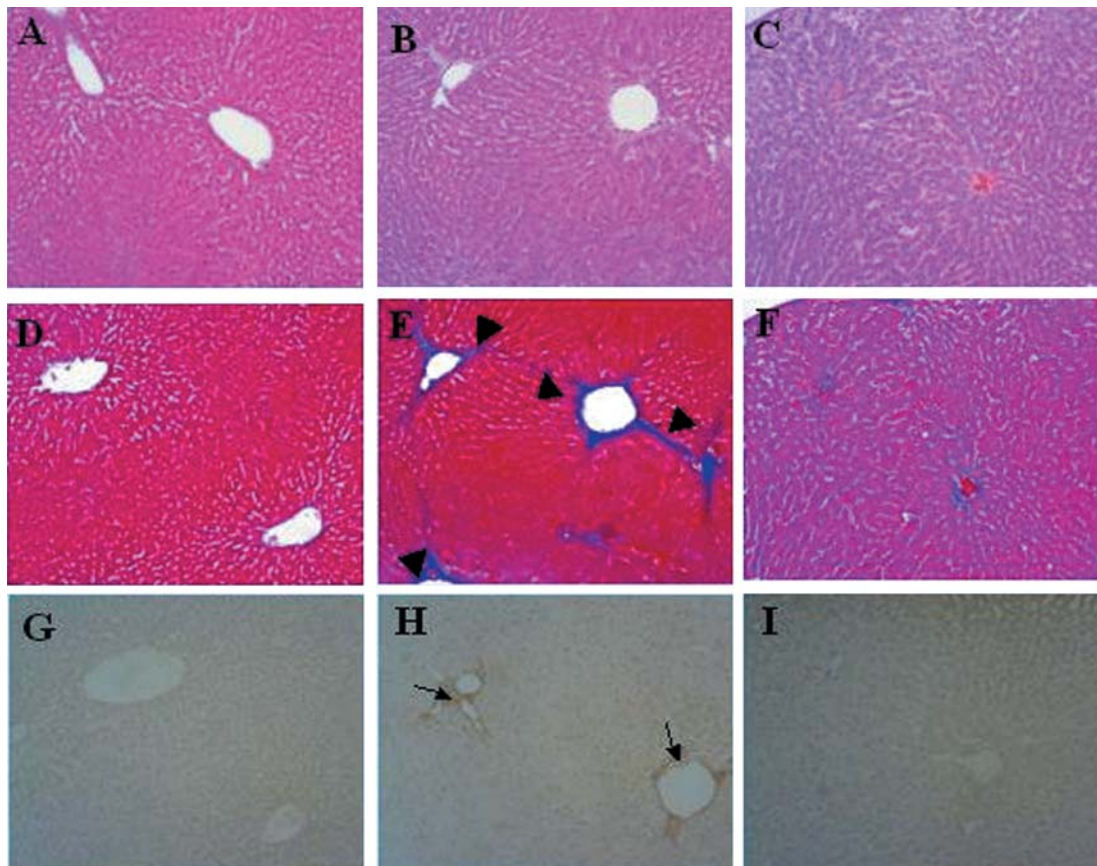


Figure 1. Hepatic fatty change and fibrosis in each of the three groups at week 4.

A, D: In control groups, normal collagen fibers in the area of portal and central vein. G: Normal α -SMA signaling. B, E: In CCl_4 groups, collagenous septa (arrowhead) forming from central vein. H: α -SMA-positive myo-fibroblast (arrow) are observed around the portal triad and central vein. C, F: Silymarin groups show almost the same lesion with the control groups. I: No detectable α -SMA. Original magnification: x33, Stain: H&E (A, B, C); Azan staining (D, E, F); α -SMA immuno-staining (G, H, I), Groups: Control (A, D, G); CCl_4 (B, E, H); Silymarin (C, F, I)

Histopathology. The same hepatic slice was examined sonographically from each rat. They were rapidly removed and fixed in freshly prepared 10% neutral buffered formalin, processed routinely, and embedded in paraffin. Sections were cut 4 μm in thickness. The sections were stained with hematoxylin and eosin (H&E) and with a special Azan stain for collagen fibers. In these experiments, the degree of fibrosis in each section of the liver was classified as a grade 0 - 4 (27).

Ratio assessment of collagen and fatty change. An image analyzer measured the collagen and fatty change ratio in the histopathological examination. We used the Azan-stained slide for each group's liver section. The ratio data were given as means and standard deviation (SD) with number of observation given. A significant difference from the control was judged by the Mann-Whitney *U*-test at $p < 0.05$ and is indicated by *.

Immunohistochemistry. Immunohistochemical studies were performed by the labelled streptavidin-biotin method using a Histostatin-plus bulk kit (Zymed Laboratories Ins., San Francisco, CA, USA). The primary antibody used was monoclonal anti - α

smooth muscle actin, at a dilution of 1:800 (clone 1A4, Sigma Co., St. Lois, MO, USA). Non-immunized goat sera, which were used instead of the primary antibody, served as a negative control.

Statistical analysis. All experimental data shown were derived from experiments repeated two or three times as indicated, unless otherwise noted. Data are expressed as mean and standard deviation (SD). Statistical analysis of the data was done using Instat Program (Graphpad Software Inc., San Diego, CA, USA). A Mann-Whitney *U*-test was conducted and the data that were considered to be significantly different were reported at probability levels of $p < 0.05$ or $p < 0.01$, as indicated by * or **.

Results

Histopathological observations. As the hepatic injuries developed to cirrhosis, the grade of hepatic fibrosis changed from grade 0 to grade 4 (Table II). In the control group, a small amount of collagen was found principally in portal areas, which was stained blue by Azan staining (Figure 1D). At week 4,

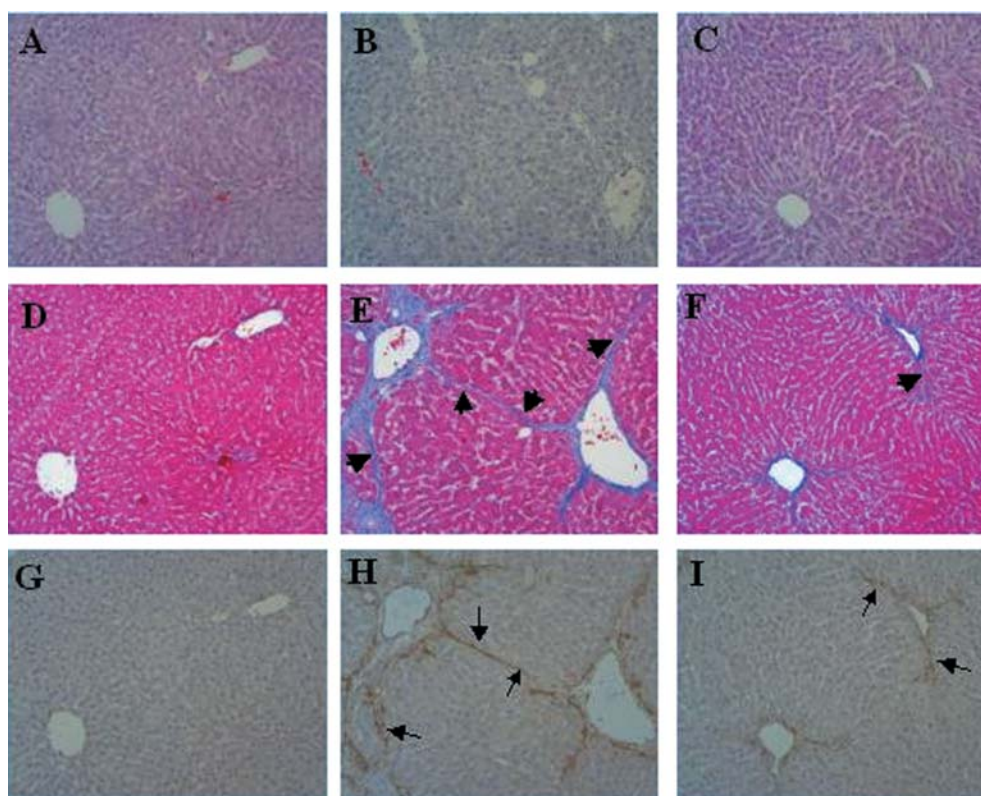


Figure 2. Hepatic fibrosis in each of the three groups at week 8. A, D: Control groups show as a normal lesion. G: Normal α -SMA signaling. B, E: In CCl_4 -treated groups, small fatty change and bridging fibrosis with collagenous septa formation (arrowhead) is mainly observed. H: MFBs expressing α -SMA (arrow) are mainly observed in the fibrous septa in CCl_4 -treated groups. C, F: In silymarin groups, severe lipid droplets are observed along the hepatic cords, and collagenous septa forming from the central vein (arrowhead). I: Weak α -SMA-positive pattern shows inhibitory fibrosis pattern. Original magnification: $\times 33$, Stain: H&E (A, B, C); Azan staining (D, E, F); α -SMA immuno-staining (G, H, I), Groups: Control (A, D, G); CCl_4 (B, E, H); Silymarin (C, F, I)

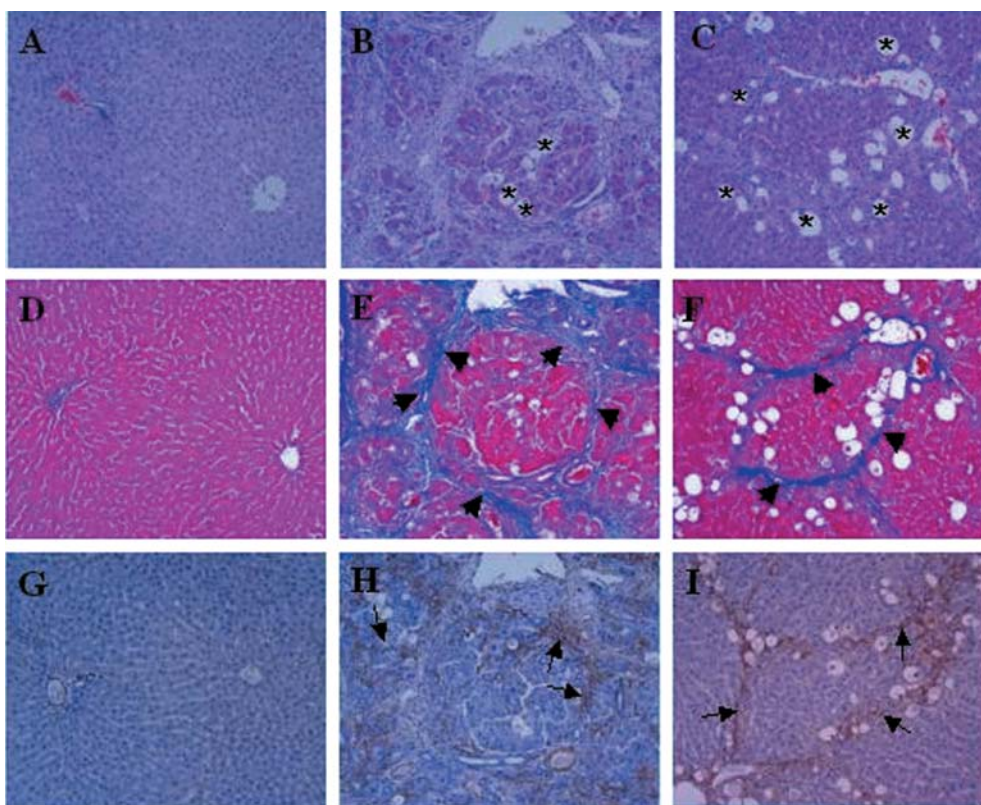


Figure 3. Hepatic fibrosis and cirrhosis in each of the three groups at week 12. A, D: Control groups show as a normal lesion. G: Normal α -SMA signaling. B, E: In CCl_4 -treated group, pseudolobulation is marked and small lobuli divided from each pseudolobuli. Collagen accumulation (arrowhead) is increased and fatty change like macrovesicular droplets rarely observed (asterisk). H, I: α -SMA-positive MFBs (arrow) are shown, with a very similar pattern of collagen accumulation. In the CCl_4 -treated group (H), α -SMA is slightly decreased, compared with the silymarin-treated group (I) C, F: In the silymarin-treated group, small pseudolobuli form with thin collagenous bridging (arrowhead) and fatty change like macrovesicular (asterisk). Original magnification: $\times 33$, Stain: H&E (A, B, C); Azan staining (D, E, F); α -SMA immuno-staining (G, H, I), Groups: Control (A, D, G); CCl_4 (B, E, H); Silymarin (C, F, I)

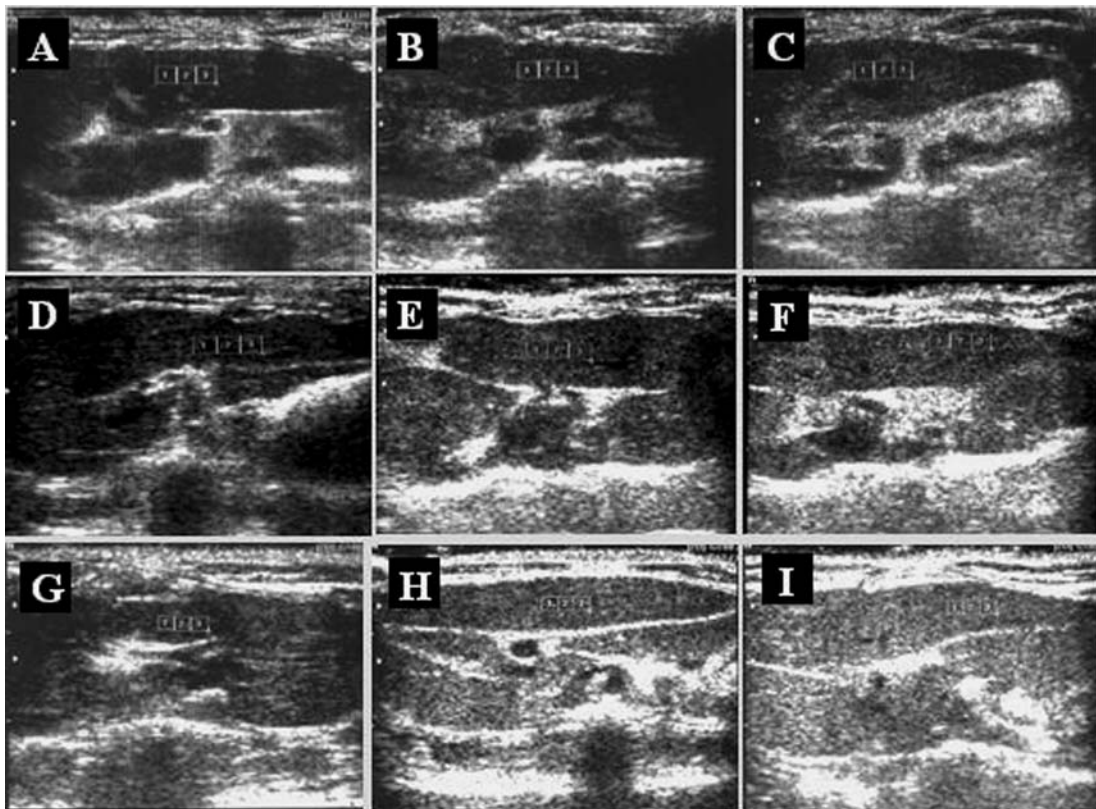


Figure 4. B-mode ultrasound images in each of the three groups. At 4 weeks, A: Control groups showed no change in the liver echogenicity. B, C: Hepatic echogenicity was increased. At 8 weeks, D: Control groups. E, F: Hyperechogenic texture of liver in the both CCl_4 - and silymarin-treated groups; the silymarin-treated group showed more echogenicity than the CCl_4 -treated groups. At 12 weeks, H, I: Echogenicity increased more than the results at 8 weeks. Brighter, coarser and more dotted shape texture in the silymarin-treated group were observed.

centrilobular necrosis and moderate fatty change of liver were found (Figure 1B) in the CCl_4 -treated only group. In this group, there was collagen accumulation, forming slender septa links between the central veins (Figure 1E). In the silymarin administration group with CCl_4 injection, mild centrilobular necrosis and fatty change were observed at 4 weeks (Figure 1C), and the presence of connective tissue was almost normal around the areas of central veins (Figure 1F). At week 8, the control group had a mild physiological fatty change around central veins (Figure 2A), but no increasing collagen accumulation and inflammatory cell infiltration were observed (Figure 2D). In the CCl_4 -treated group, fatty change was rarely observed (Figure 2B), but collagen fibers were abundant in the centrilobular area and the neighboring central veins were bridged by fibrous septa. Then, pseudolobuli were formed by thin fibrous septa (Figure 2E). In contrast, moderate to severe fatty change was detected around the periportal area and the central vein in the silymarin group (Figure 2C). A slight accumulation

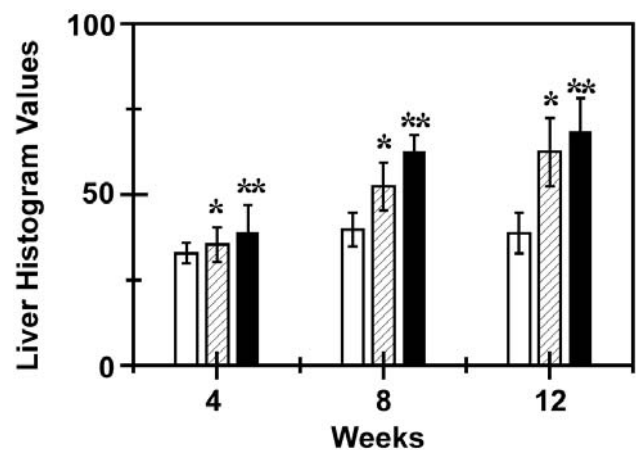


Figure 5. The comparison of the liver histogram. Each value represents mean and standard deviation (SD). Both CCl_4 - and silymarin-treated groups had statistically significant difference, compared with control group. * $p < 0.05$, ** $p < 0.01$ by Mann-Whitey U-test. Open bar: control, Hatched bar: CCl_4 , Closed bar: CCl_4 + silymarin

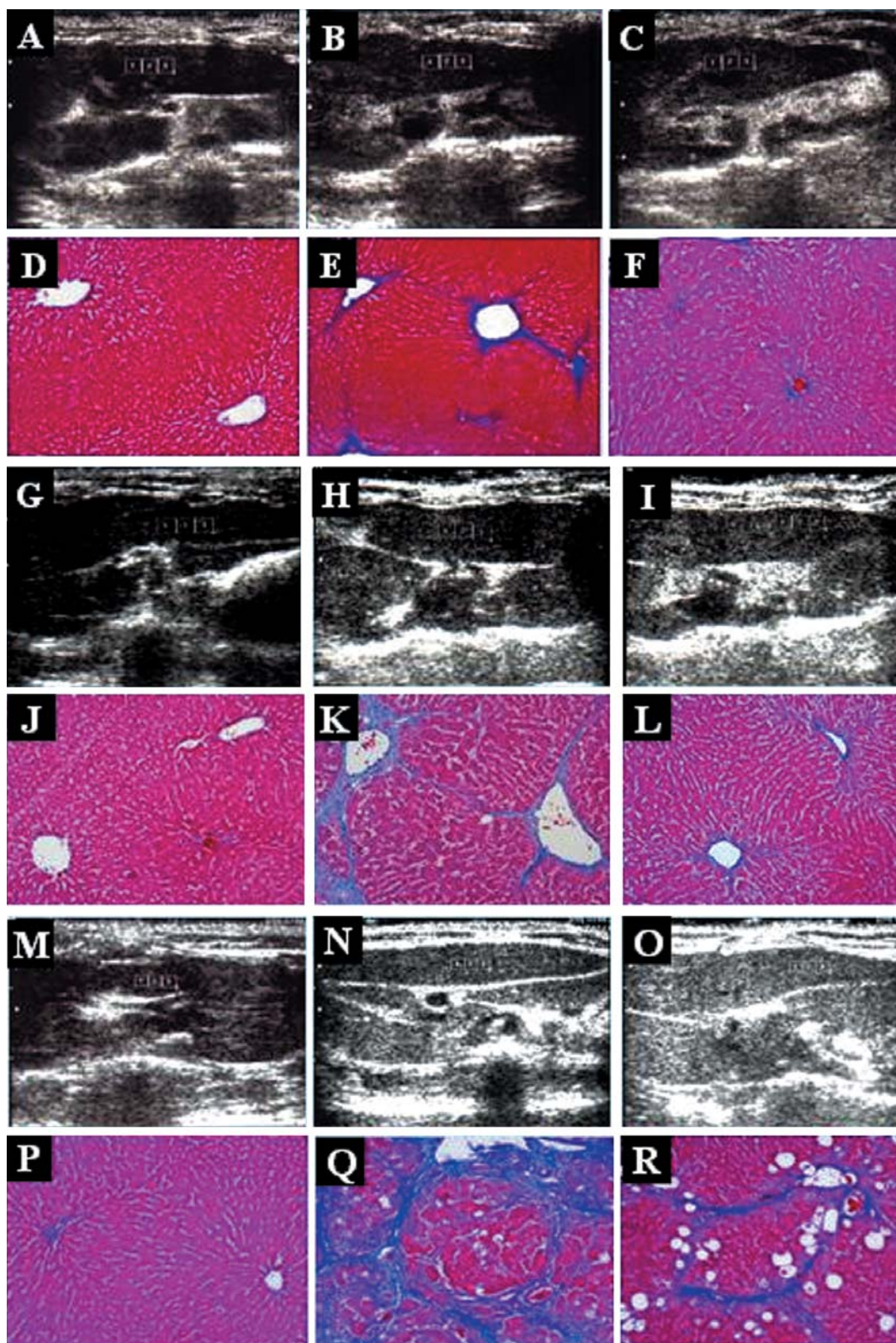


Figure 6. Comparison of B-mode ultrasound images and histopathology. A-F: 4 weeks, G-L: 8 weeks, M-R: 12 weeks. A, D, G, J, M, P: Control groups. B, E, H, K, N, Q: CCl_4 groups. C, F, I, L, O, R: CCl_4 + silymarin groups.

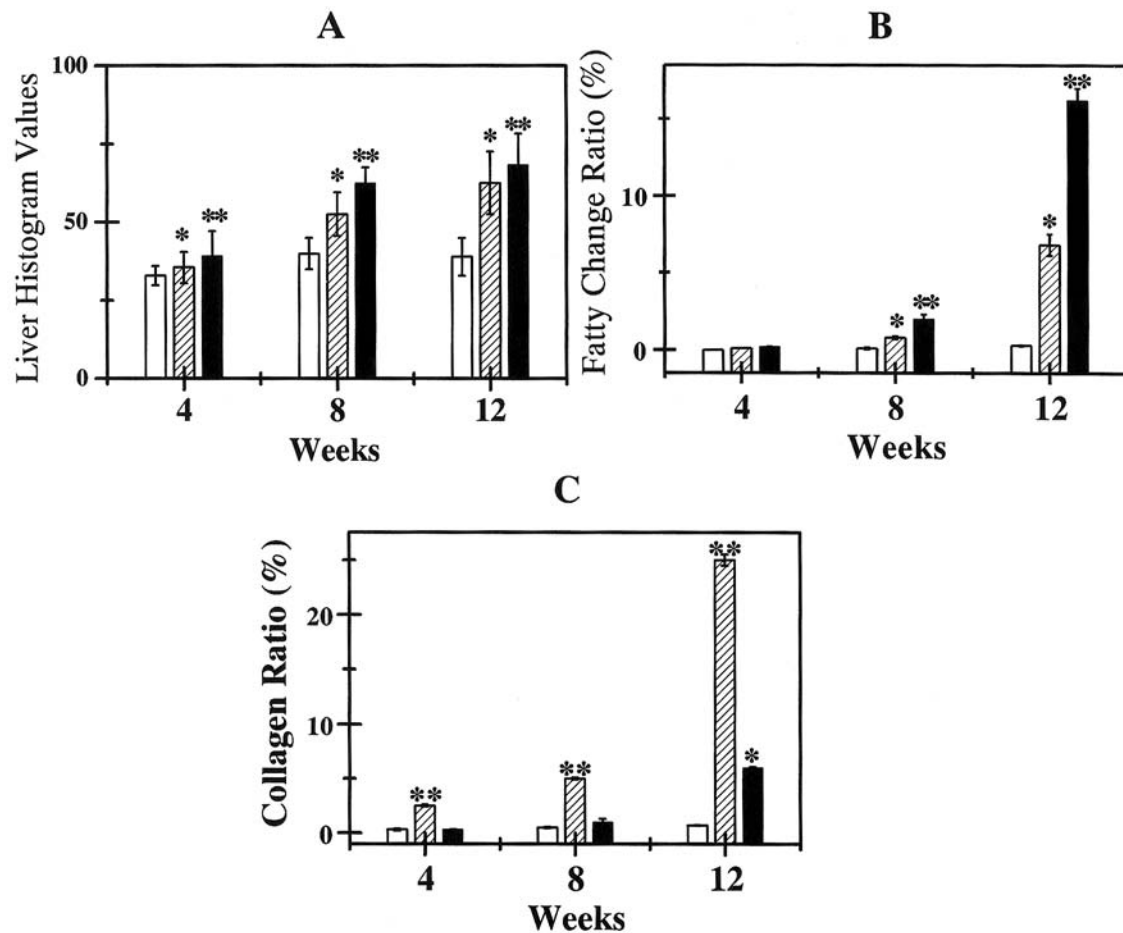


Figure 7. Comparison of B-mode liver histogram and collagen and fatty change ratio. Each value represents the mean and SD. A: B-mode histogram values. CCl₄- and silymarin-treated groups had significant values compared with control. B: Fatty change ratio. Silymarin-treated group showed significant values, compared with control and CCl₄-treated groups. C: Collagen ratio. CCl₄-treated groups showed significant difference, compared with control and CCl₄ + silymarin groups. * $p < 0.05$, ** $p < 0.01$ by Mann-Whitney U-test. Open bar: control, Hatched bar: CCl₄, Closed bar: CCl₄ + silymarin

and spread of collagen fibers around central veins, as demonstrated by Azan stain, was also observed (Figure 2F).

At week 12, the control group showed the same histopathological lesion as the results of week 8. In the CCl₄-treated group, pseudolobuli were formed actively and macrovesicular droplets were detected (Figure 3B, E). The collagenous septa were much thicker than those of the silymarin group and pseudolobuli were subdivided into smaller lobuli (Figure 3E). However, in the silymarin-treated group, large lipid accumulations were detected more than in the CCl₄-treated group and pseudolobuli were formed by thin collagenous septa (Figure 3C, F).

Immunohistochemistry. Normal expression of myofibroblasts (MFBS) was identified by α -SMA-positive staining and was limited to only the central veins and portal triad (Figure 1G,

2G). However, as liver damage progressed, α -SMA-positive cells markedly increased around the portal veins and central vein in the CCl₄-only-treated group at weeks 4 and 8 (Figures 1H, 2H). With silymarin in the CCl₄-treated group, α -SMA-positive cells were detected only around the central and portal veins, the same as in the control group at week 4 (Figure 1I). At week 8, increasing α -SMA-positive MFBS exhibited the same pattern of collagen fiber spread from the central veins (Figure 2I). However, there was an increase of α -SMA-positive cells in the CCl₄-only-treated group compared to the CCl₄ + silymarin-treated group at week 8 (Figure 2H, I). At week 12, as the CCl₄-treated group developed into the cirrhotic stage, α -SMA-positive MFBS were observed decreasing a little along the thick collagenous septa (Figure 3H), compared with week 8. The silymarin-treated group showed active expression of α -SMA as the same pattern with

fibrosis (Figure 3I), indicating expression of collagen matrix in the hepatocytes against activation of myofibroblasts, which disappeared at the stage of cirrhosis. This phenomenon has already been demonstrated in our laboratory.

Ultrasonograms. At week 4, the liver parenchyma showed hypoechogenicity in the control group (Figure 4A). However, in the CCl₄-treated group, liver echogenicity became slightly focal hyperechogenic (Figure 4B). The silymarin-treated group had a similar echo pattern as the CCl₄-treated group (Figure 4C). Thus, between the control group and CCl₄-treated group, the control and silymarin-treated group showed a significantly increased mean grey level in the histogram. However, the grey levels of the CCl₄-only-treated group and the CCl₄ + silymarin-treated group had no differences among them (Figure 4B, C).

From week 8, the hepatic parenchymal echo was more increased than that of week 4 due to aging processes (Figure 4D). In the CCl₄-treated group at week 8, the liver B-mode showed a diffuse hyperechogenic, coarse and dot-shaped pattern, but the distribution was still homogeneous (Figure 4E). A more hyperechogenic and coarse echo pattern was observed in the silymarin-treated group at week 8, compared with the CCl₄-treated group (Figure 4F). In the histogram, the mean grey levels of each group were significantly increased in the CCl₄- and silymarin-treated groups, compared with those in the control group. There were also significant differences between the CCl₄-treated group and silymarin group in mean grey levels of B-mode ultrasonography (Figure 5).

At week 12, hyperechogenicity was enhanced in both the CCl₄- and silymarin-treated groups. However, the silymarin-treated group showed a more increased echo pattern than the CCl₄-treated group (Figure 4H, C).

Comparison of histopathology and B-mode histogram. i) B-mode histogram and fatty change rate: Mild fatty change around central veins and fibrous septa appeared in the CCl₄-treated group at 4 weeks (Figure 6E). However, there was little or no collagen accumulation in the control group while the silymarin-treated group showed more infiltration fatty change than the CCl₄-treated group (Figure 6F). At 8 and 12 weeks, mean grey levels of the CCl₄-treated group were significantly increased, compared with those of the control (Figure 7B). There were also significant differences between control and silymarin + CCl₄- and CCl₄-treated groups in mean grey levels (Figure 7B). In the fatty change ratio in the Azan staining, the silymarin-treated group showed more significant infiltration of lipids, compared with the control and CCl₄ group (Figure 7C), indicating the inhibitory effects of fibrosis. ii) B- mode histogram and collagen accumulation rate: At week 4, the mean grey levels of the control-, CCl₄- only and CCl₄ + silymarin-treated

groups exhibited significant differences. The MGL of the CCl₄- only and CCl₄ + silymarin-treated groups were higher than that of the control group. However, both the CCl₄-treated group and the silymarin-treated groups showed no significance (Figure 7A). The collagen accumulation ratio (%) identified by image analysis clearly showed the similar results between the control and silymarin-treated group. However, only the CCl₄-treated group contained higher collagen amounts compared with other groups (Figure 7C).

During the progress of cirrhosis induced by CCl₄, sonogram results at 8 weeks for hepatic parenchymal grey levels were greatly changed as hyperechogenic signals (Figure 6H, I). The control group showed the lowest echogenicity, but the grey levels of the silymarin-treated groups were significantly more increased compared with the CCl₄ group (Figure 7A). However, the collagen accumulation ratio of each group was still developed and the CCl₄-treated group maintained the highest levels (Figure 7C). At 12 weeks, the B-mode histogram values were the highest in the silymarin group, but the collagen rate was highest in the CCl₄-treated group (Figure 7A, C). These results suggest that the B-mode histogram can be more affected by infiltration of lipid than by intact accumulation of collagen fibers.

Discussion

Generally, laboratory tests for liver function include glutamic-oxaloacetic transaminase (GOT), glutamic-pyruvic transaminase (GPT), albumin, total bilirubin and other pathological markers that are also evaluated routinely in most liver diseases (5, 6). However, the value of laboratory tests for diagnosing liver fibrosis are very limited, and final histopathological examination with biopsy is still the golden criterion for the diagnosis of liver fibrosis and cirrhosis in humans (28, 29). Our prospective study suggests that image analysis of the grey level histogram with B-mode ultrasound could be applicable for investigating liver cirrhosis caused by detrimental factors such as CCl₄, carcinogens and drugs (12).

Liver biopsy has traditionally been the standard method for assessing hepatic fibrosis and cirrhosis, but the procedure is invasive in nature and has a low incidence of complications (30). In our studies, we have attempted to develop a diverse diagnostic method for fibrosis and cirrhosis. The histogram of B-mode grey levels in ultrasound was evaluated for the process of fibrosis and cirrhosis, compared with diagnostic evaluation of histopathological analysis.

On the basis of the histology of chronic liver disease, the relationship between the grade and stage of histopathology and non-invasive diagnostic parameters, including B-mode ultrasound examination, has been explored. The authors reported that B-mode ultrasound provided more valuable resources than that of other imaging diagnostic methods such as CT and/or MR imaging for diagnosis of liver fibrosis (13).

At this point, we evaluated the relationship of collagen and fatty change rate in the histopathological analysis followed by grey levels of histogram. In the grey levels of the histogram, the CCl₄-treated group and silymarin-treated group compared with the control group were evaluated at a significant difference at week 4. These results suggest that fatty infiltration rates during hepatic disease lead to more significant increase in the grey levels histogram in the B-mode ultrasound than that of collagen accumulation. Our findings are similar to previous studies, although earlier researchers analyzed lipid and collagen contents with chemical methods (31).

At week 8, histopathological difference indicated the strong anti-oxidative effects of silymarin and silymarin's membrane stabilizing actions (23- 25). However, in the B-mode histogram, the grey levels of the silymarin-treated group were higher than those of the CCl₄-treated group, indicating that the fatty change rates of the silymarin-treated group were more affected than those of the CCl₄-treated groups. On the other hand, the collagen accumulation ratio was highest in the CCl₄-treated group (grade 3), even given the low grade of the B-mode histogram.

In the 12-week results, we evaluated the further relationship of liver fatty change ratio and B-mode histogram in ultrasound during the cirrhotic process by comparing increasing patterns of both in the silymarin-treated group. In the CCl₄-treated group, the collagen ratio was the highest at 8 and 12 weeks during cirrhosis, but the B-mode histogram was not well correlated with the increasing collagen ratio. Previous studies also evaluated this correlation with collagen contents in the model of CCl₄-treated and silymarin with CCl₄-treated animals (31). They reported that silymarin-treated animals had lower collagen contents in liver cirrhosis induced by CCl₄ than that of CCl₄-treated only animals (23, 31). Based on the relationship of lipid contents and echogenicity of the cirrhotic liver in B-mode histogram evaluation, ultrasound B-scan parameters include echogenicity of the liver, and not only depend on lipid contents but also on the amounts of connective tissue. However, connective tissue without lipid content is not a critical factor for the grey levels in B-mode ultrasound. According to our reproducible results, lipid content is the critical factor affecting the B-mode grey levels (31). There are general agreements with these findings that increased lipid content is the most important factor for the ultrasound signal information in the liver (32, 33).

Given the results of the current study, we reached three important conclusions. First, the grey levels histogram in B-mode ultrasonography is a useful diagnostic method in CCl₄-induced rat hepatic cirrhosis. Second, as the hepatic fibrosis developed, the B-mode of grey levels in sonography increased, depending on both the liver fatty change and collagen accumulation ratio. However, the fatty change ratio is the most important factor that affects the B-mode grey

level histogram in ultrasound. Third, we also characterized the effect of silymarin, which is noted as a hepatoprotective drug, which caused a one-step delay of progress of cirrhosis through the pathological scoring.

All these data taken together suggest that the evaluation criteria of hepatic disease such as inflammation, fibrosis and cirrhosis-like hepatic fulminant status through the B-mode grey level histogram are useful in diagnostic evaluation during the progress of liver disease and also can be applied for pharmacological screening of hepatoprotective agents in the field of biomedical science and clinical therapies.

References

- 1 Luster MI, Simeonova PP, Gallucci RM, Bruccoleri A, Blazka ME and Yucesoy B: Role of inflammation in chemical-induced hepatotoxicity. *Toxicol Lett* 120: 317-25, 2001.
- 2 Victor M and Eric O: Liver. *Pediatrics* 113: 1097-1106, 2004.
- 3 Reinhard S, Remy M and Reto B: The use of silymarin in treatment of liver disease. *Drugs* 61: 2035-2063, 2001.
- 4 Maclachlan NJ and Cullen JM: Chapter 2. Liver, biliary system, and exocrine pancreas. *In: Tomson's Special Veterinary Pathology* (Carlton WW, Zachary JF and McGavin MD, 2nd eds). Missouri, Mosby, pp. 94-96, 1995.
- 5 Thomas CJ, Ronald DH and Norval WK: Digestive system. *In: Veterinary Pathology* (6th ed). Maeyland, Lippincott Williams & Wilkins, pp. 1098-1099, 1997.
- 6 Galambos JT: Alcoholic cirrhosis (in relation with cirrhosis in general). *In: Bockus Gastroenterology* (Berk JE, 4th ed). Philadelphia, W. B. Saunders Co., pp. 3012-3049, 1985.
- 7 Nord JH: Biopsy diagnosis of cirrhosis: blind percutaneous versus guided direct vision techniques. A review. *Gastrointest Endosc* 28: 102-104, 1982.
- 8 Piccinino F, Sangnelli E, Pasquale G and Giusti G: Complications following percutaneous liver biopsy. A multicentre retrospective study on 68,276 biopsied. *J Hepatol* 2(2): 165-173, 1986.
- 9 Espinoza P, Ducot B, Pelletier G, Attali P, Buffet C and David D: Interobserver agreement in the physical diagnosis of alcoholic liver disease. *Dig Dis Sci* 32: 244-247, 1987.
- 10 Tine F, Caltagirone M, Camma C, Cottone M, Carxi A and Filippazzo MG: Clinical indicators of compensated cirrhosis: a prospective study. *In: Chronic Liver Damage* (Dianzani MU and Gentilini P, eds). Amsterdam, Elsevier, pp. 197-198, 1990.
- 11 Giorgio A, Amoroso P, Lettieri G, Fico P, De Stefano G and Finelli L: Cirrhosis: value of caudate to right lobe ratio in diagnosis with US. *Radiology* 161: 443-445, 1986.
- 12 Lu LG, Zeng MD, Li CZ, Mao YM and Wan MB: Grading and staging of hepatic fibrosis, and its relationship with non-invasive diagnostic parameters. *World J Gastroenterol* 9: 2574-2578, 2003.
- 13 Harsinghani MG and Hahn PF: Computed tomography and magnetic resonance imaging evaluation of liver cancer. *Gastroenterol Clin North Am* 31: 759-776, 2002.
- 14 Martin DR: Magnetic resonance imaging of diffuse liver diseases. *Top Magn Reson Imaging* 13: 151-163, 2002.
- 15 Hung CH, Lu SN, Wang JH, Lee CM, Chen TM, Tung HD, Chen CH, Huang WS and Changchien CS: Correlation between ultrasonographic and pathologic diagnoses of hepatitis B and C virus-related cirrhosis. *World J Gastroenterol* 38: 153-157, 2003.

- 16 Tchelepi H, Ralls PW, Radin R and Grant E: Sonography of diffuse liver disease. *J Ultrasound Med* 21: 1023-1032, 2002.
- 17 Zheng RQ, Wang QH, Lu MD, Xie SB, Ren J, Su ZZ, Cai YK and Yao JL: Liver fibrosis in chronic viral hepatitis: an ultrasonographic study. *World J Gastroenterol* 9(11): 2484-2489, 2003.
- 18 Perez TR: Is cirrhosis of the liver experimentally produced by CCl₄ an adequate model of human cirrhosis? *Hepatology* 3: 112-120, 1983.
- 19 Paquet KJ and Kamphausen U: The carbon-tetrachloride hepatotoxicity as a model of liver damage. *Acta Hepatogastroenterol* 22: 84, 1975.
- 20 Jiang Z, You DY, Chen XC and Wu J: Monitoring of serum markers of fibrosis during CCl₄-induced liver damage. Effects of antifibrotic agent. *J Hepatol* 16: 282-289, 1992.
- 21 Magliulo E, Carosi PG, Minoli L and Gorini S: Studies on the regenerative capacity of the liver in rats subjected to partial hepatectomy and treated with silymarin. *Arzneim-Forsch Drug Res* 237: 161-167, 1973.
- 22 Down WH, Chasseaud LF and Grundy RK: Effect of silybin on the hepatic microsomal drug metabolizing enzyme system in the rat. *Arzneim-Forsch Drug Res* 24: 1986-1988, 1974.
- 23 Mourelle M, Muriel P, Favari L and Franco T: Prevention of CCl₄-induced liver cirrhosis by silymarin. *Fundam Clin Pharmacol* 3: 183-191, 1989.
- 24 Muriel P, Garcia-pina T, Perez-Alvarez V and Mourelle M: Silymarin protects against paracetamol-induced lipid peroxidation and liver damage. *J App Toxicol* 12: 439-442, 1992.
- 25 Ramellini G and Meldolesi J: Stabilization of isolated rat liver plasma membranes by treatment *in vitro* with silymarin. *Arzneim Forsch* 24: 806-808, 1974.
- 26 Dehmlow C, Erhard J and de Groot H: Inhibition of Kupffer cell function as an explanation for the hepatoprotective properties of silibinin. *Hepatology* 23: 749-754, 1996.
- 27 Kobayashi N, Ito M, Nakamura J, Cai J, Gao C, Hammel JM and Fox IJ: Hepatocyte transplantation in rats with decompensated cirrhosis. *Hepatology* 31: 851-857, 2000.
- 28 Gabrielli GB, Capra F, Casaril M, Squarzone S, Tognella P, Dagradi R, De Maria E, Colombari R, Corrocher R and De Sandre G: Serum laminin and type 3 procollagen in chronic hepatitis C. Diagnostic value in the assessment of disease activity and fibrosis. *Clin Chim Acta* 265: 21-31, 1997.
- 29 Castera L, Hartmann DJ, Chapel F, Guettier C, Mall F, Lons T, Richardet JP, Grimbert S, Morassi O, Beaugrand M and Trinchet JC: Serum laminin and type 4 collagen are accurate markers of histologically severe alcoholic hepatitis in patients with cirrhosis. *J Hepatol* 32: 412-418, 2000.
- 30 Layer G, Zuna I, Lorenz A, Zerban H, Haberkorn U, Bannasch P, van Kaick G and Rath U: Computerized ultrasound B-scan texture analysis of experimental diffuse parenchymal liver disease: correlation with histopathology and tissue composition. *J Clin Ultrasound* 19: 193-201, 1991.
- 31 Bamber JC and Hill CR: Acoustic properties of normal and cancerous human liver-2 dependence on pathological condition. *Ultrasound Med Biol* 7: 121-133, 1981.
- 32 Lin T, Ophir J and Potter G: Correlation of ultrasonic attenuation with pathologic fat and fibrosis in liver disease. *Ultrasound Med Biol* 14: 729-734, 1988.
- 33 Parker KJ, Asztely MS, Lerner RM, Schenk EA and Waag RC: *In vivo* measurement of ultrasound attenuation in normal and diseased liver. *Ultrasound Med Biol* 14: 127-136, 1988.

Received July 26, 2004

Revised January 5, 2005

Accepted February 10, 2005